Agromet 39 (2): 120-130, 2025

Agromet
journal.ipb.ac.id/index.php/agromet
ISSN : 0126 - 3633

Spatiotemporal Patterns of Meteorological Drought in the National Food Barn Region: A Case Study of South Sulawesi Province

Nastiti Andini[1,2], I Putu Santikayasa[1]*, Amsari Mudzakir Setiawan[2]

[1] Department of Geophysics and Meteorology, IPB University, Bogor, Indonesia.
[2] Center for Climate Change Information, Indonesia Agency for Meteorology Climatology and Geophysics, Jakarta, Indonesia 10610.

ARTICLE INFO

Received
26 July 2025

Revised
21 November 2025

Accepted for Publication
16 December 2025

Published
31 December 2025

doi: 10.29244/j.agromet.39.2.120-130

Correspondence:
I Putu Santikayasa
Department of Geophysics and Meteorology, IPB University, Bogor, Indonesia.

Email: ipsantika@apps.ipb.ac.id

This is an open-access article distributed under the CC BY License.
© 2025 The Authors. *Agromet*

ABSTRACT

Hydrometeorological disasters, particularly droughts, pose a significant threat to food crop productivity. South Sulawesi, one of Indonesia's major rice-producing regions outside Java, is highly vulnerable to drought impacts. This study analyzes the spatiotemporal patterns of meteorological drought in South Sulawesi during 1981–2020 using the Standardized Precipitation Index (SPI) and applies run theory to characterize drought events. Monthly rainfall data were obtained from the Climate Hazards Center InfraRed Precipitation (CHIRP) dataset and complemented with ground-based observations from the BMKG rainfall observation network. Principal Component Analysis (PCA) with varimax rotation was employed to identify dominant spatial patterns of meteorological drought variability. The results identify three principal regions explaining more than 65% of the total variance: Region 1 (R1; 56%) in northern South Sulawesi, Region 2 (R2; 10%) in the central to eastern areas, and Region 3 (R3; 10%) in the western region. R1 exhibits the highest drought frequency and intensity but relatively short durations, whereas R3 shows the lowest frequency but the longest durations and largest magnitudes. A positive correlation between drought duration and magnitude is observed across all regions, along with a significant drying trend in the southern part of R2. Overall, these findings provide important insights into the spatial and temporal variability of meteorological drought in South Sulawesi and offer a scientific basis for strengthening drought risk management and regional food security strategies.

KEYWORDS

drought, principal component analysis, regionalization, standardized precipitation index, trend.

1. INTRODUCTION

Drought is one of the major drivers of food insecurity worldwide (Barrett, 2010), with its impacts felt most strongly by smallholder farmers whose livelihoods rely heavily on agricultural systems (Duffy et al., 2021; Marjuki et al., 2025). In Indonesia, drought significantly undermine agricultural productivity, and it is often associated with climate variability such as El Niño–Southern Oscillation (ENSO), and intensified under a changing climate (Arora, 2019; Gao et al., 2024). For instance, during the 1997/1998 El Niño caused a 6% decline in national rice production (Siswanto et al., 2022). These events demonstrate how drought can disrupt food systems across the country, particularly in agriculturally dependent regions.

South Sulawesi faces a high to very high risk of drought, which impacts the vulnerability of food production (Estiningtyas et al., 2020). As one of Indonesia's primary food-producing provinces, ranking among the top contributors of rice, maize, and secondary crops (Badan Pusat Statistik, 2023), climate extremes pose a serious threat to national food security. Understanding how drought occurs, varies spatially, and evolves over time is therefore essential for strengthening climate resilience in this strategic agricultural landscape.

Meteorological drought assessments commonly rely on drought indices, with the Standardized Precipitation Index (SPI) being one of the most widely used due to its simplicity, multi-timescale flexibility, and comparability across regions (Gevaert et al., 2018; Hayes et al., 2011). Short-term SPI, particularly the 3-month SPI (SPI-3), is especially relevant for agriculture

and crop-growth periods (Sgroi et al., 2021). While medium-term (12-month) and long-term (24 to 48-month) timescales are used to assess drought impacts on water resources and hydrological conditions (Azam et al., 2018; Zhang et al., 2023). Therefore, short-term SPI is more suitable than longer timescales for detecting droughts during critical growth stages of staple crops in Indonesia.

However, drought characteristics often differ sharply across space, influenced by local climate patterns, topography, and rainfall regime (Tijdeman et al., 2022). Capturing this spatial variability typically requires regionalization approaches such as Principal Component Analysis (PCA) and its rotated form, Rotated Principal Component (RPC), which enhances interpretability and yields clearer homogeneous zones (Araneda-Cabrera et al., 2021; Espinosa et al., 2019; Vicente-Serrano, 2006). In Indonesia, Empirical Orthogonal Function (EOF) analysis—synonymous with PCA— has been applied to identify spatial patterns of SPI at various timescales (Setiawan et al., 2017), yet this study did not produce explicit regional boundaries with similar drought behaviour.

Despite extensive use of SPI and PCA-based regionalization in global and national drought studies, significant knowledge gaps remain for South Sulawesi. No previous study has applied Rotated Principal Component (RPC) analysis to delineate homogeneous meteorological drought regions within the province, nor has any work combined RPC-derived zones with run theory to characterize drought duration, severity, intensity, and frequency at a regional scale (Yevjevich, 1967; Araneda-Cabrera et al., 2021; Espinosa et al., 2019). Moreover, long-term trends of SPI-3-based drought characteristics across spatially coherent zones in South Sulawesi have not been examined, limiting the ability to develop targeted early-warning systems and climate-resilient agricultural strategies.

This study aims to analyze the spatiotemporal patterns, characteristics, and long-term trends of meteorological drought in South Sulawesi from 1981 to 2020 using the 3-month Standardized Precipitation Index (SPI-3). The analysis involves three steps: (1) delineating homogeneous drought regions through Rotated Principal Component Analysis; (2) characterize-ing drought events within each region using run theory; and (3) assessing long-term drought trends using the Mann–Kendall test and Sen's slope estimator. Through this integrated approach, the study provides a comprehendsive understanding of how drought develops, varies, and evolves across South Sulawesi, offering insights that can inform early-warning systems, climate adaptation strategies, and agricultural decision-making.

2. MATERIALS AND METHODS

2.1 Study Area

South Sulawesi is located between 0°12′ to 8° S and 116°48′ to 122°36′ E, encompassing 370 islands with a total land area of approximately 45,330 km^2. Geographically, the province is bordered by West Sulawesi and Central Sulawesi to the north, Bone Bay to the east, the Flores Sea to the south, and the Makassar Strait to the west. The topography of South Sulawesi is diverse, ranging from low-lying coastal areas at sea level to highlands reaching elevations of up to 3,469 meters above sea level in Luwu Regency. South Sulawesi experiences three main rainfall patterns: Monsoonal, Equatorial, and Local as illustrated in (Figure 1). These patterns are influenced by a variety of factors, including differences in topography and surface features (Aldrian and Dwi Susanto, 2003). The monsoonal rain type is prevalent in most of South Sulawesi. The equatorial rain type can be found in southern Luwu, southern Enrekang, most of Sidrap, Sopeng, and northern Wajo. Meanwhile, the local rain type occurs in parts of Sidrap, southern Wajo, the east coast of Bone, Bantaeng, and southern Bulukumba.

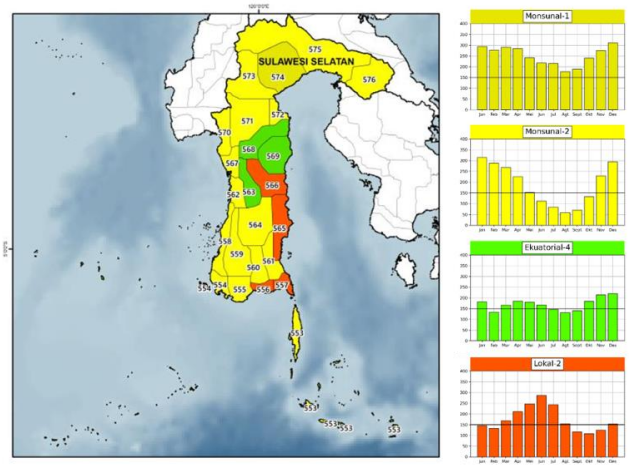

Figure 1. Map of the research location and the type of rainfall pattern observed in that area.

2.2 Datasets

The Climate Hazards Group InfraRed Precipitation (CHIRP) is a satellite-based rainfall dataset developed by the University of California, Santa Barbara in collaboration with the U.S. Geological Survey (USGS) (Funk et al., 2015). Monthly rainfall data in this study were obtained from the CHIRP+Pos dataset, which combines CHIRP satellite-based rainfall estimates with ground-based observations provided by the Indonesian Meteorological, Climatological, and Geophysical Agency (BMKG) (BMKG, 2022, 2021).

The version of CHIRP+Pos used in the study incorporated data from 1,152 rainfall stations across Indonesia and covered the period from 1982 to 2018.

A more recent version released by (BMKG, 2022) expands the dataset to include approximately 3,100 rainfall stations and covers the period from 1991 to 2020. In this study, a total of 197 rainfall stations located in South Sulawesi were used, based on the metadata of the updated CHIRP+Pos dataset. The CHIRP+Pos dataset has a spatial resolution of 0.05° (~5 km²) and covers the temporal range from 1981 to 2020. Comparative studies have shown that CHIRP+Pos provides improved rainfall estimates across most regions of Indonesia compared to the Climate Hazards Group InfraRed Precipitation with Station (CHIRPS) dataset. CHIRPS is a combination of CHIRP data with rainfall observations from several public data sources. Previous research has demonstrated that the CHIRPS dataset is capable of detecting meteorological drought in South Sulawesi using the 3-month Standardized Precipitation Index (SPI-3), yielding correlation coefficients ranging from 0.4 to 0.8 when compared with ground observation data (A. M. Setiawan et al., 2017). These findings support the reliability of satellite-merged datasets such as CHIRP+Pos for drought monitoring and climatological studies in Indonesia.

2.3 Drought indices

Drought indices are essential tools for drought management systems, providing a quantitative basis for analyzing past droughts and forecasting future events (Van Loon, 2015). The precipitation deficit can first lead to meteorological drought, which can then trigger other types of droughts, such as agricultural, hydrological, and socioeconomic droughts. Several indices are available for assessing meteorological drought, including the Standardized Precipitation Index (SPI) (McKee et al., 1993). This study used the Standardized Precipitation Index (SPI) as the drought index, because it's benefit.

SPI timescales correspond to different drought processes. To align with the research objectives, a 3-month timescale SPI (SPI-3) was utilized to capture short-term drought conditions relevant to agricultural impacts. The SPI-3 was computed by first fitting the monthly rainfall data to a gamma probability distribution, which was then transformed into a normal distribution (Mishra and Singh, 2010). Once converted to a normal distribution, the SPI has a mean of 0, enabling direct comparison across different locations and time periods. Negative SPI values indicate drier-than-normal conditions, with values below -1 used as the threshold for identifying drought events in this analysis. The length of the rainfall dataset significantly influences the scale parameters and the shape of the gamma distribution (Wu et al., 2005). Therefore, it is essential to use rainfall data of equal length across all study locations to ensure consistency and comparability in the SPI calculation.

This study applied run theory (Yevjevich, 1967) at a critical level of -1.0 SPI to identify and analyze drought characteristics, enabling easier statistical comparisons of drought parameters. Five drought characteristics were analyzed: duration, magnitude, intensity, severity, and frequency. While the definitions of drought duration and frequency were largely consistent across the literature, definitions of severity, magnitude, and intensity varied. Drought duration was defined as the time from the onset to the offset of a drought period, and drought frequency referred to the number of drought events within a specified timeframe (Le et al., 2019; McKee et al., 1993; Yevjevich, 1967). This study adopted the definitions of intensity and magnitude proposed by (Faiz et al., 2023; McKee et al., 1993). Drought intensity was defined as the peak SPI deficit during a single drought event, while magnitude referred to the total cumulative SPI deficit over the drought period. Although some studies define intensity as the ratio of SPI total deficit to drought duration (Li et al., 2021; Mishra and Singh, 2010; Sattar and Kim, 2018), this study used that ratio to define drought severity.

2.4 Rotated principal component

Principal Component Analysis (PCA) has emerged as a valuable method for identifying dominant drought patterns and assessing spatial variability. PCA was performed on the SPI-3 time series to identify homogeneous drought regions and to characterize the spatiotemporal patterns of meteorological drought (Araneda-Cabrera et al., 2021; Espinosa et al., 2019). The SPI-3 matrix for the period 1981–2020 was analyzed by computing the covariance matrix. From this matrix, eigenvalues and eigenvectors were derived to determine the principal components (PCs), which represent dominant modes of drought variability across the study area. The number of selected PCs was determined based on cumulative variance thresholds, which vary depending on research objectives. Previous studies have applied different thresholds, such as 40% (Le et al., 2019), 60% (Bouguerra et al., 2024), 75% (Araneda-Cabrera et al., 2021), and 80% (Espinosa et al., 2019). The choice of threshold depends on standard "rules of tumb" (Cangelosi and Goriely, 2007), specific needs of the research, the interpretation of cumulative variance, and personal considerations. In this study, the selection criterion required the cumulative variance explained by the selected PCs to be at least 65%, with each subsequent component contributing more than 5% to ensure meaningful regional differentiation.

Following the identification of PCs, a varimax orthogonal rotation was applied to enhance the interpretability of the spatial patterns—an approach known as Rotated Principal Component (RPC) analysis (Araneda-Cabrera et al., 2021; Espinosa et al., 2019; Vicente-Serrano, 2006). The results of the RPC are then correlated with the SPI-3 values for each research grid, facilitating smoother boundaries in the regionalization. A correlation threshold of 0.55 was adopted to assign grid points to drought regionalization, ensuring complete coverage of the study area. The determination of this correlation value varies based on specific research needs. Increasing threshold results in overlapping regions, while decreasing it causes certain areas to be excluded from any regional grouping. For instance, in Mozambique, a limit of 0.6 is applied (Araneda-Cabrera et al., 2021), while in Madeira Island, a limit of 0.65 is used (Espinosa et al., 2019). In contrast, studies in northern Algeria have not applied a fixed correlation threshold for regionalization (Bouguerra et al., 2024).

2.5 Trend analysis

This research employed the Mann-Kendall test as a non-parametric test. The Mann-Kendall test is commonly utilized in the analysis of environmental and climate data due to their robustness and flexibility, especially when the data did not follow a normal distribution (Hidayat et al., 2025; Kocsis et al., 2017; Ramos and Cordeiro, 2013). These tests were particularly valuable for detecting temporal trends and remained reliable even in the presence of missing data points (Ramos and Cordeiro, 2013). Previous research demonstrated the effectiveness of the Mann-Kendall test in analyzing drought trends, as shown in studies conducted in Vietnam (Le et al., 2019), northern Algeria (Bouguerra et al., 2024), and Mozambique (Araneda-Cabrera et al., 2021). In addition to the Mann-Kendall test, this study also employed Sen's slope estimator (Sen, 1968) to calculate the rate of change in drought magnitude over time for the identified trends. The Mann-Kendall and Sen's slope tests were applied to the SPI-3 across the entire research grid.

3. RESULTS AND DISCUSSION

3.1 Drought regionalization

A total of approximately 1,480 SPI-3 time series were analyzed using Principal Component Analysis (PCA) to examine their spatiotemporal characteristics, as described in the Methods section. The matrix used for PCA consisted of 480 rows, representing monthly SPI-3 values from 1981 to 2020, and 1,480 columns, corresponding to the grid points derived from CHIRP+Pos data over South Sulawesi.

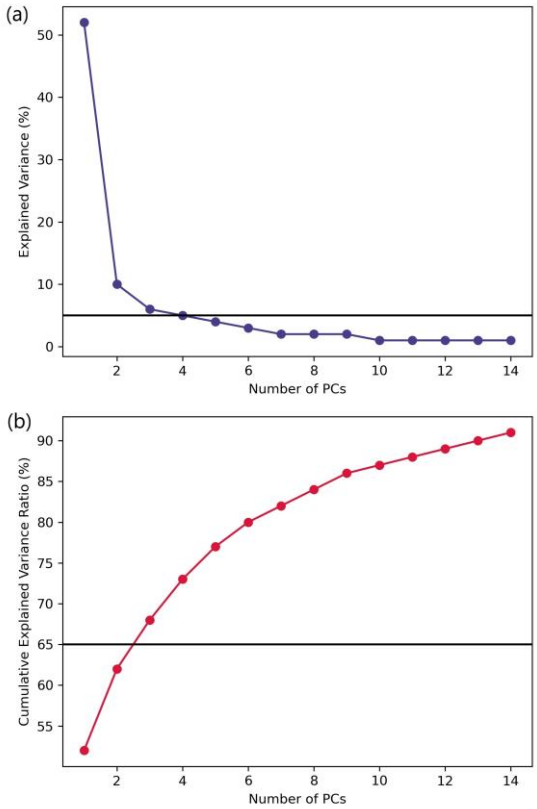

Figure 2. (a) Number and (b) cumulative of variance for principal component of the SPI3.

Based on the criteria outlined in method section, three PCs were selected (Figure 2). The first PC consistently accounted for the highest percentage of variance, followed by the second and third, aligning with previous studies (Bouguerra et al., 2024; Espinosa et al., 2019). In this analysis, PC1 accounted for 52% of the explained variance, while PC2 and PC3 contributed 10% and 6%, respectively, resulting in a total cumulative variance of 68%. PC4, which accounted for only 5% of the variance, did not meet the inclusion criteria and was therefore excluded from further analysis. The selection of these 3 PCs matched the number of rainfall patterns in South Sulawesi: monsoonal, equatorial, and local.

In addition to the SPI- 3 dataset, PCA was also applied to SPI-6, SPI-9, and SPI-12 datasets; however, the results are not presented in this paper (See Figure A1). The cumulative variances for the first three principal components of SPI-6, SPI-9, and SPI-12 were 70%, 70%, and 71%, respectively, with PC4 consistently contributing 5%—a pattern similar to that observed in the SPI-3 analysis.

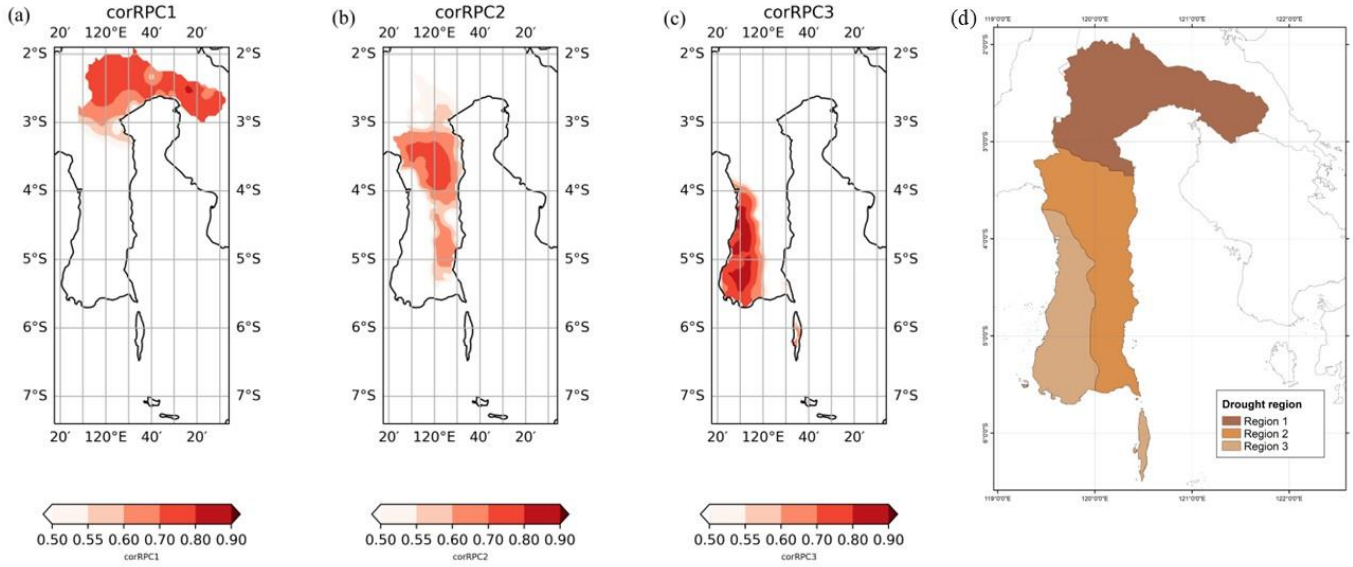

Figure 3. Spatial distribution of coefficient correlation between SPI-3 and (a) RPC1, (b) RPC2, and (c) RPC3. (d) drought regions based on correlation between each RPCs and SPI-3.

To enhance the interpretability of spatial distribution of the homogeneous region SPI-3, a Rotated Principal Component (RPC) analysis is conducted using varimax orthogonal rotation of the predetermined PCs. The results of this analysis yield component loading values, which represent the correlation coefficients between each RPC and SPI-3. Figure 3 (a, b, and c) illustrates the spatial distribution regions of correlation threshold of 0.55 between each RPC and SPI-3 values. While this threshold is chosen to ensure sufficient correlation values, avoiding overlapping areas or uncovered regions remains challenging. In regions with overlapping correlation values, the selected region is determined by the higher correlation value. For regions without any correlation value, the selection is based on the region with more property similarity factors.

Figure 3 (d) presents the spatial distribution of the drought regions following certain adjustments. The area has been divided into three regions: Region 1 (R1) in the northern part, Region 2 (R2) in the central to southern area, and Region 3 (R3) in the western part. R1 included East Luwu, North Luwu, Palopo City, North Toraja, northern Tana Toraja, and northern Luwu. R2 comprised southern Tana Toraja, southern Luwu, northern Pinrang, Enrekang, most of Sidrap, Wajo, eastern Sopeng, most of Bone, Sinjai, and Bulukumba. R3 consisted of southern Pinrang, Pare-Pare City, small part of Sidrap, Barru, western Sopeng, small part of Bone, Pangkajene, Maros, Makassar City, Gowa, Takalar, Jeneponto, Bantaeng, and Selayar.

The spatial patterns identified through RPC corresponded with the three main rainfall regimes in South Sulawesi—monsoonal, equatorial, and local. Although the number of selected principal components is the same as the number of rainfall patterns in South Sulawesi, it does not imply that the areas represented by PC1, PC2, and PC3 will correspond to each rainfall pattern. R1 and R3 were predominantly influenced by monsoonal rainfall, while R2 reflected a combination of all three types. These findings suggest that the observed drought variability in R1 and R3 is likely driven by similar climatic mechanisms during both the rainy and dry seasons, particularly the seasonality associated with monsoonal precipitation. This can be attributed to the fact that R1 and R3 are primarily affected by the same type of rainfall, specifically monsoonal precipitation.

A similar study on drought variability in Vietnam found that 2 out of the 3 selected PC exhibited similar drought variability characteristics, this was possible due to differences in climate conditions in the other PC (Le et al., 2019). This study contributes to the broader understanding of how localized climatic regimes influence drought behavior and emphasizes the importance of considering spatial heterogeneity when assessing drought risk. The identification of these distinct regions provides a basis for more targeted drought monitoring and mitigation strategies in South Sulawesi.

3.1 Spatial Distribution of Drought Characteristics

Following the identification of meteorological drought regionalization, this section presents the spatial distribution of drought characteristics based on run theory applied to the defined regions. Figure 4 displays the spatial patterns of five meteorological drought characteristics in South Sulawesi. The shortest drought durations were observed in the southern part of R2 (Bulukumba) and R3 (Soppeng), with values of 1.8

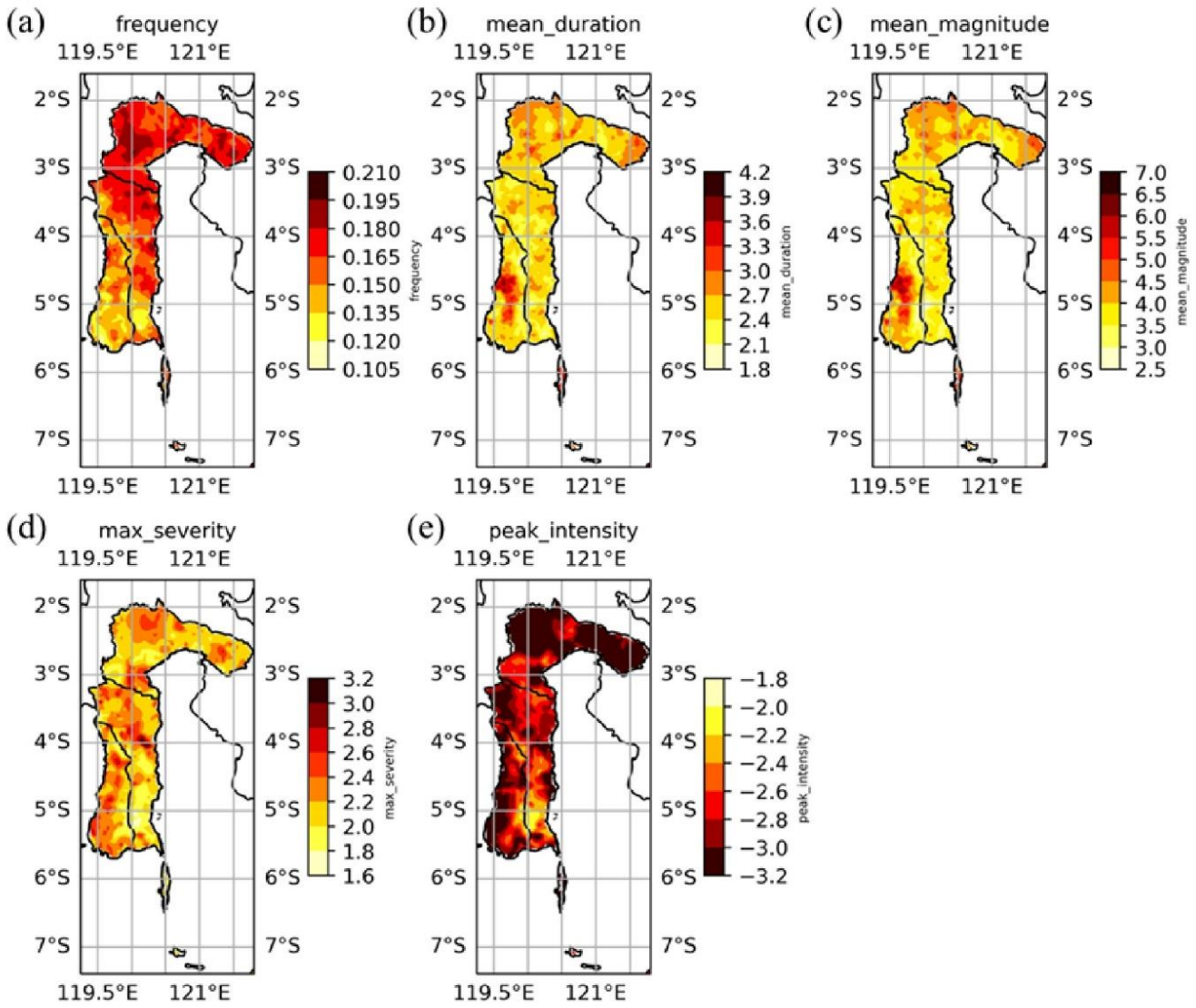

Figure 4. Spatial distribution of five meteorological drought characteristics: (a) drought frequency, (b) mean duration (months), (c) mean magnitude, (d) maximum severity, and (e) peak intensity.

months, while the longest durations occurred in R3 (southern Barru and Pangkajene), with values of 3.9 months. The lowest drought magnitudes were recorded in Bone (R2 and R3), with values of 2.5, while the highest magnitude was found in R3 (southern Barru and Pangkajene) with a value of 6.5.

Figure 4 shows that R3 experienced the longest and shortest drought durations also the highest and the lowest drought magnitudes compared to other regions. This finding reveal that R3 experienced both the widest range of drought durations and magnitudes, indicating substantial variability across locations. The observed relationship between drought duration and magnitude—where longer droughts result in greater cumulative precipitation deficits—is consistent with prior research (Espinosa et al., 2019). While R3 recorded the highest duration and magnitude, R1 also displayed an area with high duration and magnitude over a fairly wide region. In contrast, R1 and R2 exhibited more consistent drought durations, with fewer occurrences of very short or very long events, suggesting greater temporal uniformity. This relative stability in R1 and R2 may reflect a more regular climatic regime, whereas the pronounced variability in R3 highlights greater challenges for regional water resource and drought management.

R3, specifically Jeneponto, exhibited the lowest drought frequency, with a value of 0.11. In contrast, the highest drought frequency was observed in R1, particularly in North Luwu, with a value of 0.21. Overall, R1 experienced drought events more frequently than other regions, as indicated by its relatively narrow range of drought frequency values. The lowest peak intensity, with a value of 2, were recorded in Bone and Sinjai (R2) and Bone (R3). In contrast, higher peak intensity was consistently observed in R1, characterized by a relatively narrow range of intensity values. Prolonged droughts may not occur as frequently as

short-term events, but their extended duration allows for the accumulation of more severe hydrological deficits, increasing the likelihood of long-term environmental and agricultural impacts. This finding is further supported by (Jiao et al., 2021), who emphasized that droughts of moderate intensity, when sustained over a long period, tend to have more persistent negative effects on the environment than shorter but more intense droughts. Importantly, the impact of drought duration and intensity on recovery processes can vary depending on the type of vegetation involved.

Furthermore, Research has shown a contrasting pattern between the duration and frequency of droughts in R3 and R1. This pattern suggests that in regions where droughts tend to last longer, they occur less frequently. This finding aligns with previous studies (Faiz et al., 2023; Ge et al., 2016), reinforcing the understanding that drought characteristics are interdependent and must be analyzed collectively rather than in isolation.

R2 was found to experience high-severity droughts despite their shorter durations. the potential risk for agricultural systems, particularly when such events coincide with critical crop growth stages could lead to devastating consequences (Rippey, 2015; Sgroi et al., 2021). In contrast, R3, with moderate severity but longer durations, presents risks to ecological systems and long-term water supply, a concern also documented in other drought-prone areas (AghaKouchak et al., 2015; Gabriel and Kreutzwiser, 1993; Zhang et al., 2018).

The combination of long mean duration, high peak intensity, large mean magnitude, and low frequency is observed in R3, particularly in Pangkajene, southern Barru, and Selayang. This indicates that while droughts are less frequent in these areas compared to other regions, when they do occur, they tend to last for an extended period and possess a significant overall drought strength. This pattern reflects the complexity of drought dynamics in coastal and monsoon-affected regions and supports similar observations in Argentina, where infrequent but extreme droughts have been reported (Sgroi et al., 2021). Collectively, these findings contribute new insights into the spatial heterogeneity of drought impacts in South Sulawesi and underscore the value of region-specific drought monitoring and mitigation strategies.

3.2 Spatiotemporal Distribution of Drought Trends

Identifying trends in drought analysis is crucial for understanding long-term changes in water availability. This understanding supports effective water resource management and agricultural planning, ultimately contributing to food security. In this study, trend analysis was performed on the regionalized SPI-3 time series for the period 1981–2020 using the Mann-Kendall test. Figure 5 presents the spatial distribution of the monthly SPI-3 trends over the period 1981–2020 for each research grid. Historical drought trends show diverse patterns across regions throughout the study period. The analysis showed varying drought trends across the study area. An increasing trend in SPI-3 was observed in eastern East Luwu within R1, with a statistically significant rate ranging from 0.001 to 0.003 per month, indicating wetter conditions. In contrast, significant decreasing trends in SPI-3 were detected in several areas, including southern Bone, eastern Gowa, Sinjai, and northern Bulukumba, with rates between -0.001 and -0.005 per month.

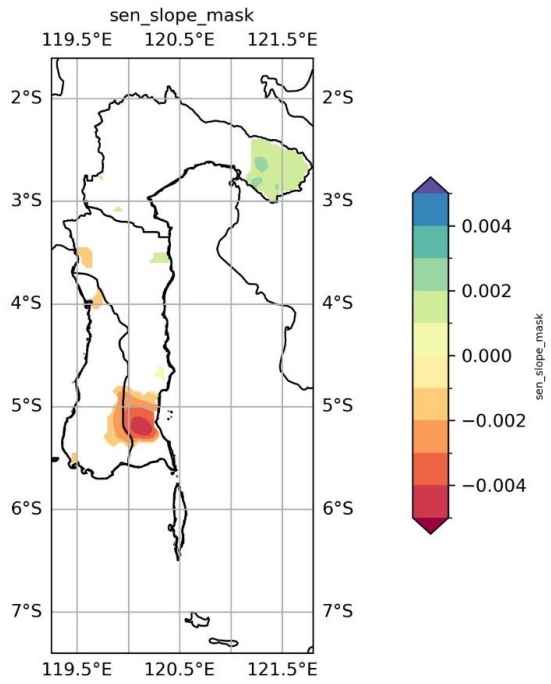

Figure 5. Spatial distribution for sen's slope of SPI-3. White region means the p-value greater than 0.05 or not significant.

These findings provide insight into the spatial variability of drought trends across South Sulawesi and highlight the need for region-specific adaptation strategies. Notably, several areas within R1 that exhibit a wetting trend are located near or around existing lakes. This spatial correlation raises the possibility of a hydrological connection between the presence of lakes and the observed increase in wetness. Further investigation is needed to assess whether these lakes influence local moisture regimes or serve as indicators of shifting hydrological patterns in the region. When compared to previous research conducted in northern Algeria using the SPI-3 (Bouguerra et al., 2024), the magnitude of the trends observed in this study is lower.

In Algeria, the slopes of R1, R2, and R3 represented by RPC1, RPC2, and RPC3 ranged from −0.0021 to −0.0035, whereas in South Sulawesi, the maximum positive slope was approximately 0.001. This comparison suggests that while South Sulawesi is experiencing changes in drought patterns, the rate of change is less pronounced than in other semi-arid regions, potentially due to differences in climatic regimes or geographic influences.

4. CONCLUSION

This study aimed to investigate the spatiotemporal patterns, characteristics, and trends of meteorological drought in South Sulawesi using the 3-month Standardized Precipitation Index (SPI-3) from 1981 to 2020. By applying Rotated Principal Component (RPC) analysis, three homogeneous drought regions were identified, each corresponding to distinct rainfall regimes. The RPC divided South Sulawesi into three regions: RPC1 corresponds to Region 1 (R1), located in the northern part; RPC2 corresponds to Region 2 (R2), situated in the central to southern part; and RPC3 corresponds to Region 3 (R3), found in the western part of South Sulawesi. R1 experienced the highest drought frequency and intensity, R2 showed the highest severity with short duration and low magnitude, and R3 exhibited the longest duration and largest magnitude but the lowest frequency, intensity, and severity. Mann-Kendall trend analysis revealed a wetting trend in R1 and a drying trend in R2. These findings contribute to the understanding of regional drought behavior in tropical monsoonal climates and provide valuable insights for drought mitigation and agricultural planning. However, a limitation of this study is its focus solely on meteorological drought, without incorporate-ing agricultural or hydrological drought impacts. Future research should explore multi-type drought assess-ments and examine the relationship between drought patterns and rainfall regimes in greater detail to enhance regional water resource management strategies.

ACKNOWLEDGEMENTS

This study was supported and funded by Indonesia Endowment Fund for Education Agency (LPDP) - The Ministry of Finance Republic Indonesia. The authors appreciate Indonesia Agency for Meteorology Climatology and Geophysics (BMKG) for providing the data for this study.

REFERENCES

AghaKouchak, A., Feldman, D., Hoerling, M., Huxman, T., Lund, J., 2015. Water and climate: Recognize anthropogenic drought. Nature 524, 409–411. https://doi.org/10.1038/524409a

Aldrian, E., Dwi Susanto, R., 2003. Identification of three dominant rainfall regions within Indonesia and their relationship to sea surface temperature. International Journal of Climatology 23, 1435–1452. https://doi.org/10.1002/joc.950

Araneda-Cabrera, R.J., Bermudez, M., Puertas, J., 2021. Revealing the spatio-temporal characteristics of drought in Mozambique and their relationship with large-scale climate variability. Journal of Hydrology: Regional Studies 38, 100938. https://doi.org/10.1016/j.ejrh.2021.100938

Arora, N.K., 2019. Impact of climate change on agriculture production and its sustainable solutions. Environmental Sustainability 2, 95–96. https://doi.org/10.1007/s42398-019-00078-w

Azam, M., Maeng, S.J., Kim, H.S., Lee, S.W., Lee, J.E., 2018. Spatial and Temporal Trend Analysis of Precipitation and Drought in South Korea. Water 10. https://doi.org/10.3390/w10060765

Badan Pusat Statistik, 2023. Statistik Indonesia 2023.

Barrett, C.B., 2010. Measuring Food Insecurity. Science 327, 825–828. https://doi.org/10.1126/science.1182768

BMKG, 2022. Pemutakhiran Zona Musim Indonesia Periode 1991-2020. Pusat Informasi Perubahan Iklim BMKG.

BMKG, 2021. Peta rata-rata curah hujan dan hari hujan periode 1991 –2020 Indonesia. Pusat Informasi Perubahan Iklim BMKG.

Bouguerra, H., Derdous, O., Tachi, S.E., Hatzaki, M., Abida, H., 2024. Spatiotemporal investigation of meteorological drought variability over northern Algeria and its relationship with different atmospheric circulation patterns. Theoretical and Applied Climatology 155, 1507–1518. https://doi.org/10.1007/s00704-023-04705-9

Cangelosi, R., Goriely, A., 2007. Component retention in principal component analysis with application to cDNA microarray data. Biology Direct 2, 2. https://doi.org/10.1186/1745-6150-2-2

Duffy, C., Toth, G.G., Hagan, R.P.O., McKeown, P.C., Rahman, S.A., Widyaningsih, Y., Sunderland, T.C.H., Spillane, C., 2021. Agroforestry contributions to smallholder farmer food security in Indonesia. Agroforestry Systems 95, 1109–1124. https://doi.org/10.1007/s10457-021-00632-8

Espinosa, L.A., Portela, M.M., Rodrigues, R., 2019. Spatio-temporal variability of droughts over past 80 years in Madeira Island. Journal of Hydrology: Regional Studies 25, 100623. https://doi.org/10.1016/j.ejrh.2019.100623

Estiningtyas, W., Perdinan, Rahman, A., Suciantini, 2020. Adaptation strategy for sustainable food sovereignty based on vulnerability and climate risk assessment : a case study of Sulawesi Island. IOP Conference Series: Earth and Environmental Science 484, 012072. https://doi.org/10.1088/1755-1315/484/1/012072

Faiz, M.A., Zhang, Y., Tian, X., Zhang, X., Ma, N., Aryal, S., Naz, F., 2023. Time series analysis for droughts characteristics response to propagation. International Journal of Climatology 43, 1561–1575. https://doi.org/10.1002/joc.7933

Funk, C., Peterson, P., Landsfeld, M., Pedreros, D., Verdin, J., Shukla, S., Husak, G., Rowland, J., Harrison, L., Hoell, A., Michaelsen, J., 2015. The climate hazards infrared precipitation with stations—a new environmental record for monitoring extremes. Scientific Data 2, 150066. https://doi.org/10.1038/sdata.2015.66

Gabriel, A.O., Kreutzwiser, R.D., 1993. DROUGHT HAZARD IN ONTARIO: A REVIEW OF IMPACTS, 1960–1989, AND MANAGEMENT IMPLICATIONS. Canadian Water Resources Journal 18, 117–132.

Gao, Y., Zhu, D., Wang, Z., Lin, Z., Zhang, Y., Wang, K., 2024. Projected Increasing Negative Impact of Extreme Events on Gross Primary Productivity During the 21st Century in CMIP6 Models. Earth's Future 12, e2024EF004798. https://doi.org/10.1029/2024EF004798

Ge, Y., Apurv, T., Cai, X., 2016. Spatial and temporal patterns of drought in the Continental U.S. during the past century. Geophysical Research Letters 43, 6294–6303. https://doi.org/10.1002/2016GL069660

Gevaert, A.I., Veldkamp, T.I.E., Ward, P.J., 2018. The effect of climate type on timescales of drought propagation in an ensemble of global hydrological models. Hydrology and Earth System Sciences 22, 4649–4665. https://doi.org/10.5194/hess-22-4649-2018

Hayes, M., Svoboda, M., Wall, N., Widhalm, M., 2011. The Lincoln Declaration on Drought Indices: Universal Meteorological Drought Index Recommended. Bulletin of the American Meteorological Society 92, 485–488. https://doi.org/10.1175/2010BAMS3103.1

Hidayat, R., Apip, Dasril, A.P., Taufik, M., 2025. Climate teleconnection triggers prolonged dry season in tropical maritime continent. Theor Appl Climatol 156, 626. https://doi.org/10.1007/s00704-025-05852-x

Jiao, T., Williams, C.A., De Kauwe, M.G., Schwalm, C.R., Medlyn, B.E., 2021. Patterns of post-drought recovery are strongly influenced by drought duration, frequency, post-drought wetness, and bioclimatic setting. Global Change Biology 27, 4630–4643. https://doi.org/10.1111/gcb.15788

Kocsis, T., Kovács-Székely, I., Anda, A., 2017. Comparison of parametric and non-parametric time-series analysis methods on a long-term meteorological data set. Central European Geology Central European Geology 60, 316–332. https://doi.org/10.1556/24.60.2017.011

Le, P.V.V., Phan-Van, T., Mai, K.V., Tran, D.Q., 2019. Space–time variability of drought over Vietnam. International Journal of Climatology 39, 5437–5451. https://doi.org/10.1002/joc.6164

Li, J., Wang, Y., Li, Y., Ming, W., Long, Y., Zhang, M., 2021. Relationship between meteorological and hydrological droughts in the upstream regions of the Lancang–Mekong River. Journal of Water and Climate Change 13, 421–433. https://doi.org/10.2166/wcc.2021.445

Marjuki, M., Koesmaryono, Y., Santikayasa, I.P., Sopaheluwakan, A., 2025. Assessing the Influence of Climate Services and Climate Change Adaptation Strategies on Smallholder Agriculture: A Systematic Literature Review. Agromet 39, 75–85. https://doi.org/10.29244/j.agromet.39.2.75-85

McKee, T.B., Doesken, N.J., Kleist, J., 1993. The Relationship of Drought Frequency and Duration to Time Scales. Am. Meteorol. Soc. 179–184.

Mishra, A.K., Singh, V.P., 2010. A review of drought concepts. Journal of Hydrology 391, 202–216. https://doi.org/10.1016/j.jhydrol.2010.07.012

Ramos, M.R., Cordeiro, C., 2013. Trend tests in time series with missing values: A case study with imputation. AIP Conference Proceedings 1558, 1909–1912. https://doi.org/10.1063/1.4825905

Rippey, B.R., 2015. The U.S. drought of 2012. Weather and Climate Extremes 10, 57–64. https://doi.org/10.1016/j.wace.2015.10.004

Sattar, M.N., Kim, T.-W., 2018. Probabilistic characteristics of lag time between meteorological and hydrological droughts using a Bayesian model. Terr. Atmos. Ocean. Sci. 29, 709–720.

Setiawan, A. M., Koesmaryono, Y., Faqih, A., Gunawan, D., 2017. Observed and blended gauge-satellite precipitation estimates perspective on meteorological drought intensity over South Sulawesi, Indonesia. IOP Conference Series: Earth and Environmental Science 54, 012040. https://doi.org/10.1088/1755-1315/54/1/012040

Setiawan, A.M., Lee, W., Rhee, J., 2017. Spatio-temporal characteristics of Indonesian drought related to El Niño events and its predictability using the multi-model ensemble. International Journal of Climatology 37, 4700–4719.

Sgroi, L.C., Lovino, M.A., Berbery, E.H., Müller, G.V., 2021. Characteristics of droughts in Argentina's core crop region. Hydrology and Earth System Sciences 25, 2475–2490. https://doi.org/10.5194/hess-25-2475-2021

Siswanto, S., Wardani, K.K., Purbantoro, B., Rustanto, A., Zulkarnain, F., Anggraheni, E., Dewanti, R., Nurlambang, T., Dimyati, M., 2022. Satellite-based meteorological drought indicator to support food security in Java Island. PLOS ONE 17, e0260982. https://doi.org/10.1371/journal.pone.0260982

Tijdeman, E., Blauhut, V., Stoelzle, M., Menzel, L., Stahl, K., 2022. Different drought types and the spatial variability in their hazard, impact, and propagation characteristics. Natural Hazards and Earth System Sciences 22, 2099–2116. https://doi.org/10.5194/nhess-22-2099-2022

Van Loon, A.F., 2015. Hydrological drought explained. WIREs Water 2, 359–392. https://doi.org/10.1002/wat2.1085

Vicente-Serrano, S.M., 2006. Differences in Spatial Patterns of Drought on Different Time Scales: An Analysis of the Iberian Peninsula. Water Resources Management 20, 37–60. https://doi.org/10.1007/s11269-006-2974-8

Wu, H., Hayes, M.J., Svoboda, 2005. The effect of the length of record on the standardized precipitation index calculation. Int.J.Climatol 25, 505–520.

Yevjevich, V.M., 1967. An Objective Approach to Definitions and Investigations of Continental Hydrologic Droughts. Hydrological Papers 23, 1913–2006. https://doi.org/10.1016/j.jhydrol.2009.11.013

Zhang, Y., Feng, X., Wang, X., Fu, B., 2018. Characterizing drought in terms of changes in the precipitation–runoff relationship: a case study of the Loess Plateau, China. Hydrology and Earth System Sciences 22, 1749–1766.

Zhang, Y., Wang, P., Chen, Y., Yang, J., Wu, D., Ma, Y., Huo, Z., Liu, S., 2023. The optimal time-scale of Standardized Precipitation Index for early identifying summer maize drought in the Huang-Huai-Hai region, China. Journal of Hydrology: Regional Studies 46, 101350. https://doi.org/10.1016/j.ejrh.2023.101350

ANNEX

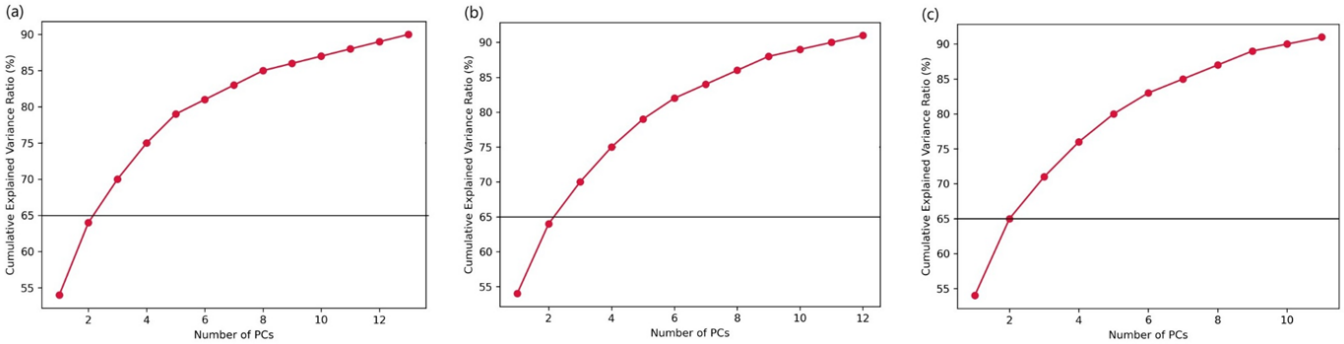

Figure A1. Cumulative explained variance (%) of the principal components for (a) SPI-6, (b) SPI-9, and (c) SPI-12. The horizontal line indicates the 65% cumulative variance threshold used to determine the number of retained principal components.